

# Thermal/Photo Conversion of Silver 4-Nitrobenzoate to Nitro/Amine-Terminated Silver Nanoparticles

Yeoung Uk Seo, Seung Joon Lee, and Kwan Kim\*

Laboratory of Intelligent Interfaces, School of Chemistry and Molecular Engineering,  
Seoul National University, Seoul 151-742, Korea

Received: August 14, 2003; In Final Form: February 4, 2004

We have investigated the thermal and photochemical characteristics of silver 4-nitrobenzoate (Ag-4NBA) using various analytical tools, such as, X-ray diffraction (XRD), diffuse reflectance infrared Fourier transform spectroscopy, Raman spectroscopy, thermogravimetric analysis, scanning electron microscopy, and transmission electron microscopy. The XRD pattern was composed of a series of peaks that could be indexed to ( $0k0$ ) reflections of a layered structure. Upon heating the sample, structural changes took place particularly at two specific temperatures. The binding state of the carboxylate group changed from bridging to unidentate at  $\sim 380$  K. A second dramatic structural change occurred at  $\sim 590$  K, producing 4NBA-capped Ag nanoparticles. The latter transition temperature for Ag-4NBA is about 80 K higher than that for silver alkanecarboxylates, and such enhanced thermal stability of Ag-4NBA must be associated with the conjugation of the carboxylate group to the aromatic ring. On the other hand, Ag-4NBA was readily subjected to photolysis even by visible radiation. Under irradiation by a He/Ne laser at 632.8 nm, 4-NBA-capped Ag nanoparticles were produced from Ag-4NBA. Upon irradiation by an Ar<sup>+</sup> laser at 514.5 nm, nitro-to-amine group conversion took place consecutively, finally producing 4-aminobenzoate-capped Ag nanoparticles. Accordingly, the Raman spectrum of Ag-4NBA taken using the 514.5-nm line as the excitation source became identical to the surface-enhanced Raman scattering (SERS) spectrum of 4-NBA adsorbed on Ag.

## 1. Introduction

Several surface-enhanced Raman scattering (SERS) studies regarding the physicochemical properties of aromatic nitro molecules on silver have been reported in the literature.<sup>1</sup> Upon irradiation by an Ar<sup>+</sup> laser, the SERS peaks of the original nitro molecules usually decline in intensity, and a new set of peaks appears. The new peaks rapidly increase in intensity as a function of the laser illumination time, suggesting that the nitro molecules are subjected to photoreaction on the silver surface. On the basis of these observations, we have recently reexamined the SERS characteristics of 4-nitrobenzenethiol (4-NBT)<sup>2a,b</sup> and 4-nitrobenzoic acid (4-NBA)<sup>2c</sup> on silver, and their SERS spectral features were found to be surprisingly coincident with those of 4-aminobenzenethiol (4-ABT) and 4-aminobenzoic acid (4-ABA) on Ag, respectively. Much the same conclusion could be derived from X-ray photoelectron spectroscopy measurements as well as from a coupling reaction forming amide bonds.<sup>2a</sup> The surface-induced photoreaction thereby allowed us to prepare patterned binary monolayers on Ag that would show different chemical reactivities. Using the binary monolayers as a lithographic template, we could also conduct site-specific chemical reactions.<sup>2a</sup>

In the past decade, the number of organic–inorganic hybrid materials that exhibit alternating 2-D molecular assemblies of organic and inorganic constituents have expanded considerably, encompassing a host of technologically relevant materials.<sup>3</sup> Silver alkanecarboxylates (AgCO<sub>2</sub>R) are one class of organic–inorganic heterostructured materials that show a well-developed progression of intense X-ray reflections; these intense X-ray

reflections are associated with the three-dimensionally stacked silver carboxylate layers.<sup>4</sup> As a result of the specific arrangement of Ag atoms in a layer, AgCO<sub>2</sub>R materials have been proposed to possess 2-D conductivity in the solid state.<sup>5</sup> AgCO<sub>2</sub>R materials are also known to decompose (in an atmosphere of N<sub>2</sub>) into alkanecarboxylate-derivatized silver nanoparticles.<sup>4d,4f</sup> Perfluorocarboxylate-stabilized silver nanoparticles have similarly been prepared via the thermal decomposition of layered silver perfluorocarboxylates.<sup>6</sup> Because the organic moieties anchored on the Ag nanoparticles can be completely removed by heating to 750 K or higher, optically tunable, SERS-active Ag films can be reproducibly fabricated on glass microscope slides.<sup>7</sup>

In conjunction with the above implications, we report herein the structure and thermal behavior as well as the photoresponse of silver 4-nitrobenzoate (Ag-4NBA). The first concern in this work is whether a layered structure is also assumed for silver aromatic carboxylate. The second concern is to determine, if it consists of a layered structure, how much the thermal characteristics of such a hybrid material are affected by the incorporation of aromatic rings instead of hydrocarbon chains. If organic molecule-derivatized Ag nanoparticles are also produced by the thermal decomposition of Ag-4NBA, the third concern is to determine whether the organic moiety is 4-nitrobenzoate; the conversion of silver compounds to silver nanoparticles must occur via a redox process; it must then be of interest to find out whether the nitro group is also converted to an amine, along with the silver species. The fourth concern is whether photoreaction occurs even for Ag-4NBA. In fact, we found that Ag-4NBA consisted of a layered structure, and 4NBA-derivatized Ag nanoparticles were produced by the thermal treatment of Ag-4NBA similarly as for silver alkanecarboxylates. Surpris-

\* Author to whom all correspondence should be addressed. Phone: +82-2-8806651. Fax: +82-2-8743704. E-mail: kwankim@plaza.snu.ac.kr.

ingly, however, 4-aminobenzoate (4ABA)-derivatized Ag nanoparticles were produced upon irradiation by an Ar<sup>+</sup> laser (at 514.5 nm) on Ag-4NBA, whereas 4NBA-derivatized Ag nanoparticles were produced by irradiation with a He/Ne laser at 632.8 nm.

## 2. Experimental Section

**2.1. Chemicals and Synthesis.** Silver nitrate (99+%), 4-nitrobenzoic acid (4-NBA, 99+%), 4-aminobenzoic acid (4-ABA, 99%), and triethylamine (99+) were purchased from Aldrich and used as received. Unless specified, other chemicals were reagent grade, and triply distilled water (resistivity greater than 18 M $\Omega$ ·cm) was used throughout. To prepare silver 4-nitrobenzoate (Ag-4NBA), a methanolic solution of AgNO<sub>3</sub> (0.1 M, 100 mL) was added dropwise to an equimolar 1:1 mixture of 4-NBA and triethylamine in methanol (100 mL). After 2 h of vigorous stirring, the resulting white solid was filtered, washed thoroughly with water and methanol, and finally dried in a vacuum; hereafter it will be called Ag-4NBA. The results of the elemental analysis, performed at the Korea Basic Science Institute using a CE instruments/ThermoQuest Model Flash EA1112 elemental analyzer, are as follows. Anal. Calcd for Ag-4NBA (%): C, 30.68; H, 1.47; O, 23.36; N, 5.11. Found: C, 30.94; H, 1.56; O, 24.05; N, 5.58. In order to help interpret the IR and Raman spectral peaks of Ag-4NBA, diffuse reflectance infrared Fourier transform (DRIFT) and SERS spectra were obtained for 4-NBA and 4-ABA self-assembled on powdered Ag (Aldrich, 99%, 2–3.5  $\mu$ m) in 10 mM methanolic solution for 3 h.

**2.2. Characterization.** XRD patterns were obtained on a Rigaku Model D/Max-3C powder diffractometer for a  $2\theta$  range of 5° to 80° at an angular resolution of 0.02° using Cu K $\alpha$  (1.5419 Å) radiation. The samples were spread on antireflection glass slides to give uniform films. A scanning electron microscope (SEM) image of Ag-4NBA was measured using a JSM 840-A scanning electron microscope at 20 kV. Transmission electron microscope (TEM) images were acquired for Ag-4NBA after thermal and radiation treatment on a JEM-2000EXII transmission electron microscope at 200 kV after placing a drop of chloroform/methanol (9:1) mixed solution on carbon-coated copper grids (200 mesh). Thermogravimetric analysis (TGA) data were obtained with a TA Instrument 2050 thermogravimetric analyzer in a nitrogen atmosphere at a heating rate of 10 K/min.

Infrared spectra were measured using a Bruker IFS 113v FT-IR spectrometer equipped with a globar light source and a liquid N<sub>2</sub>-cooled wide-band mercury cadmium telluride detector. To record the DRIFT spectra, a diffuse reflection attachment (Harrick Model DRA-2CO) designed to use 6:1, 90° off-axis ellipsoidal mirrors subtending 20% of the 4 $\pi$  solid angle was fitted to the sampling compartment of the FT-IR spectrometer. The pure powdered sample was transferred to a 4-mm diameter cup without compression and leveled by a gentle tap. A reaction chamber, made of stainless steel (Harrick Model HVC-DR2) and loaded with the powdered sample, was located inside the reflection attachment. CaF<sub>2</sub> crystals were used as infrared transparent windows. The temperature of the sampling cup was regulated using a homemade temperature controller, and the chamber was flushed continuously with dry nitrogen (ca. 10 mL/min) during the measurement of DRIFT spectra. A total of 32 scans was measured in the range of 3500–1000 cm<sup>-1</sup> at a resolution of 4 cm<sup>-1</sup> using previously scanned pure KBr as the background. The temperature of the sampling cup was raised at a rate of 10 K/min and kept for 5 min at each specified

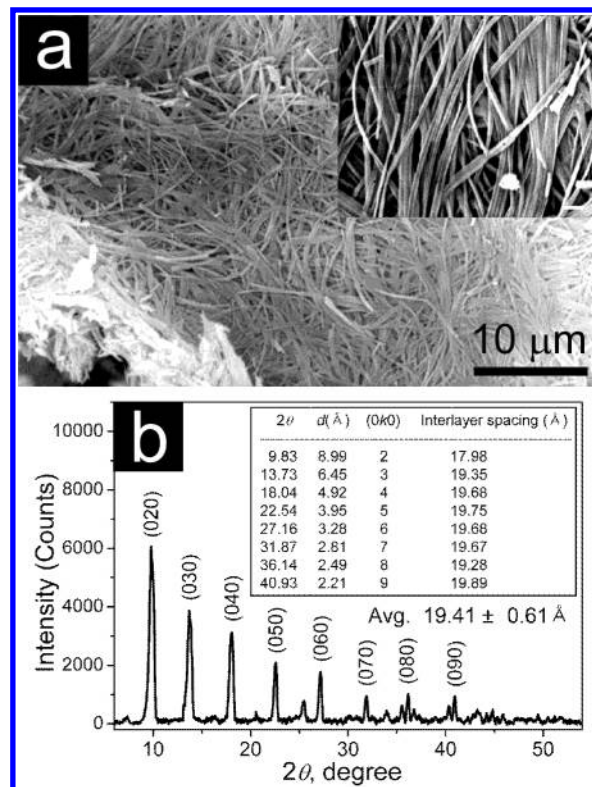


**Figure 1.** (a) SEM image of silver 4-nitrobenzoate. (b) XRD pattern of silver 4-nitrobenzoate. The interlayer spacings derived from different reflections are listed in the inset.

temperature for the acquisition of the DRIFT spectra. The Happ–Genzel apodization function was used in Fourier transforming all the interferograms. The DRIFT spectra are reported as  $-\log(R/R_0)$ , where  $R$  and  $R_0$  are the reflectance of the sample and of the pure KBr, respectively.

Raman spectra were obtained using a Renishaw Raman system model 2000 spectrometer equipped with an integral microscope (Olympus BH2-UMA). The 514.5-nm radiation from a 17 mW air-cooled Ar<sup>+</sup> laser (Spectra Physics model 163-C4210) or the 632.8-nm radiation from a 17 mW air-cooled He/Ne laser (Spectra Physics Model 127) was used as the excitation source. Raman scattering was detected with 180° geometry using a peltier-cooled (−70 °C) CCD camera (400 × 600 pixels). A glass capillary (KIMAX-51) with an outer diameter of 1.5–1.8 mm was used as a sampling device, but when it was needed to reduce photolysis, samples made into pellets were spun at 3000 rpm during the Raman spectral measurement. The data acquisition time was usually 90 s. The holographic grating (1800 grooves/mm) and the slit permitted a spectral resolution of 1 cm<sup>-1</sup>. The Raman band of a silicon wafer at 520 cm<sup>-1</sup> was used to calibrate the spectrometer, and the accuracy of the spectral measurement was estimated to be better than 1 cm<sup>-1</sup>. The Raman spectrometer was interfaced to an IBM-compatible PC, and the spectral data were analyzed using Renishaw WiRE software, version 1.2, based on the GRAMS/32C suite program (Galactic Industries).

## 3. Results and Discussion

**3.1. Structure of Silver 4-Nitrobenzoate.** The SEM image in Figure 1a reveals that Ag-4NBA has a fibrous morphology. These fibrous samples were identified as possessing a layered structure from the XRD data shown in Figure 1b. The XRD pattern shows a well-developed progression of intense reflections, and these intense reflections can be interpreted in terms

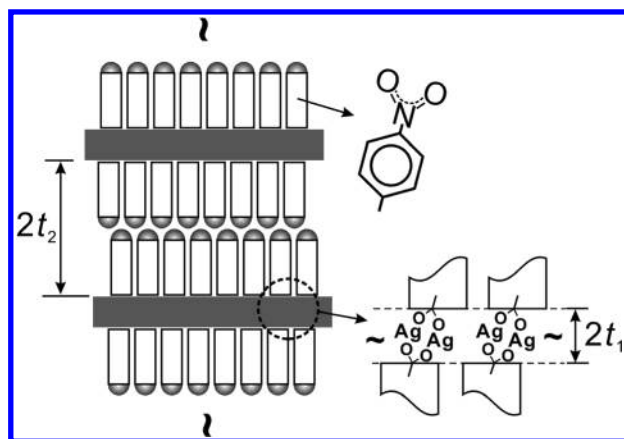


**Figure 2.** Schematic depiction of the layered silver 4-nitrobenzoate.

of three-dimensionally stacked silver carboxylate layers with a large interlayer lattice dimension.<sup>4</sup> This implies that, as in silver alkanecarboxylates, each layer of Ag-4NBA is separated from the neighboring layer by twice the length of the nitrobenzene moiety. In this sense, all intense reflections can be indexed as  $(0k0)$ , and the reflections are assigned in Figure 1b. In the inset of Figure 1b, we list the interlayer spacings derived from different reflections. The averaged interlayer spacing is  $19.41 \pm 0.61$  Å. The layered structure of Ag-4NBA is schematically drawn in Figure 2.

The comparable XRD patterns of Ag-4NBA and silver alkanecarboxylate suggest that the arrangement of silver and carboxylate must be similar to each other in the two compounds. In this light, it is informative to recall the Ag K-EXAFS study of Tolochko et al.,<sup>4c</sup> which showed that the silver atoms in silver stearate (Ag-STA) are bridged by the carboxylate in the form of dimers in an eight-membered ring and that the dimers are further bonded to each other by longer Ag-O bonds forming four-membered rings; the reported bond lengths are  $r(\text{Ag}-\text{Ag}) = 2.90$  Å,  $r(\text{Ag}-\text{O}) = 2.25$  Å,  $r(\text{C}-\text{O}) = 1.20$  Å, and  $r(-\text{OOC}-\text{CH}_2-) = 1.54$  Å. On the other hand, according to the photographic X-ray study conducted by Blakeslee and Hoard,<sup>8</sup> the bond lengths in silver perfluorobutyrate are  $r(\text{Ag}-\text{Ag}) = 2.90$  Å,  $r(\text{Ag}-\text{O}) = 2.24$  Å,  $r(\text{C}-\text{O}) = 1.25$  Å, and  $r(-\text{OOC}-\text{CF}_2-) = 1.54$  Å. When these values are used, the thickness of the Ag-COO slab, that is,  $2t_1$  in Figure 2, is estimated to be 4.83 Å. Considering that the averaged interlayer spacing derived from Figure 1b was 19.41 Å, the thickness of the nitrobenzene layer, that is,  $2t_2$  in Figure 2, should then be 14.58 Å.

Consulting the crystal structure of 4-NBA<sup>9</sup> and the van der Waals (vdW) radius of the oxygen atom,<sup>10</sup> the molecular length from the carboxylate carbon to the terminal  $\text{NO}_2$  group should be 7.73 Å. Doubling this value yields 15.46 Å, which is 0.88 Å longer than that derived from the measured XRD data, that is, 14.58 Å. The discrepancy of 0.88 Å is presumed to be due to the tilting of 4-NBA (by  $\sim 19^\circ$ ) with respect to the Ag plane and/or the interpenetration of  $\text{NO}_2$  groups between the adjacent layers in Ag-4NBA. We cannot derive the intralayer structure because of the insufficient signal-to-noise ratio for the high-angle XRD peaks, but the overall structure of Ag-4NBA as drawn in Figure 2 is presumably similar to that of silver alkanecarboxylate.

Room temperature DRIFT spectral features indicate that the as-prepared Ag-4NBA is not contaminated with free acid (see the Supporting Information). In addition, referring to the empirical relationship between the frequency difference of the carboxylate stretching bands, that is,  $\Delta\nu$  ( $\sim 190$   $\text{cm}^{-1}$ ) =  $\nu_{\text{as}}(\text{COO}^-) - \nu_{\text{s}}(\text{COO}^-)$ <sup>11,12</sup> and the types of bonding, the

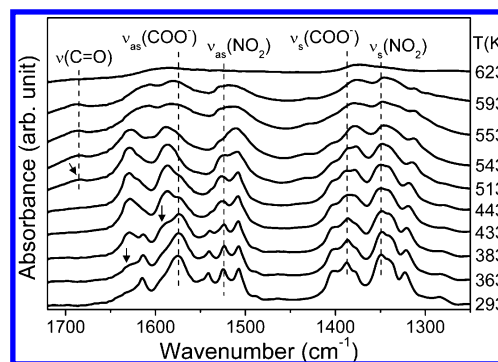


**Figure 3.** DRIFT spectra of silver 4-nitrobenzoate in the temperature range of 293–623 K. The arrows denote the occurrence of distinct spectral changes.

binding state of the carboxylate group to silver in Ag-4NBA is presumed to be a bridging one.

**3.2. Thermal Behavior of Silver 4-Nitrobenzoate.** One aim of this work was to determine how much the thermal characteristics of layered  $\text{AgCO}_2\text{R}$  would be affected by the incorporation of an aromatic ring instead of a simple alkane chain. In this regard, we have conducted a temperature-dependent DRIFT spectroscopy study along with TGA measurements.

**3.2.1. Temperature-Dependent DRIFT Spectral Pattern of Ag-4NBA.** Figure 3 shows a series of DRIFT spectra obtained as a function of temperature for Ag-4NBA. The peak positions of the carboxylate stretching bands provide information on the effect of temperature on the headgroup structure. In this light, it is informative that the  $\nu_{\text{as}}(\text{COO}^-)$  peak at  $1575$   $\text{cm}^{-1}$  is rather invariant up to 383 K and then becomes weak and disappears above 443 K. Instead, a new peak develops at  $1591$   $\text{cm}^{-1}$  from 383 K and is sustained up to 593 K. On the other hand, the  $\nu_{\text{s}}(\text{COO}^-)$  band decreases gradually from room temperature up to 623 K and the  $\nu(\text{C}=\text{O})$  band develops around 513 K. The present observation suggests that two distinct structural changes take place, one at 383 K and the other at 513 K, in connection with the Ag-O binding state. Assigning the newly developing peak at  $1591$   $\text{cm}^{-1}$  at 383 K to  $\nu_{\text{as}}(\text{COO}^-)$ , the binding state of the carboxylate group must change from bridging to unidentate at 383 K. On the other hand, free acid seems to be produced at 513 K probably from the thermal decomposition of Ag-4NBA; the first mass loss commences at  $\sim 520$  K in the TGA measurement (vide infra). It is intriguing that the  $\nu(\text{C}=\text{O})$  band due to free acid is identified at a somewhat lower temperature for silver alkanecarboxylates, that is, at 500 K for Ag-STA<sup>4d</sup> and at 480 K for silver hydroxyhexadecanoate.<sup>4f</sup> This implies that the Ag-O bonds in Ag-NBA are stronger than those in silver alkanecarboxylates, presumably because of the conjugation of the carboxylate group with the aromatic benzene ring. On the other hand, considering the melting point of pure 4-NBA (512–514 K), the observed spectral change at 513 K must also be associated with the disordering of nitrobenzene moieties.

The  $\text{NO}_2$  group related peaks also exhibit temperature-dependent spectral changes. Namely, both the  $\nu_{\text{s}}(\text{NO}_2)$  and  $\nu_{\text{as}}(\text{NO}_2)$  bands in Figure 3 gradually lose intensity from room temperature up to 623 K along with experiencing moderate band broadening. Concomitantly, the ring vibration at  $1615$   $\text{cm}^{-1}$ , that is, 8a, gradually weakens up to 443 K. A new peak, however, develops at  $1630$   $\text{cm}^{-1}$  from 363 K and is sustained up to 543 K. It then shifts to lower frequency above 553 K and becomes weak until it disappears above 593 K. The origin of the new peak at  $1630$   $\text{cm}^{-1}$  is currently unclear but its position is close to that of the 8a mode; the position of the 8a mode may be dependent on the type of bonding of the carboxylate

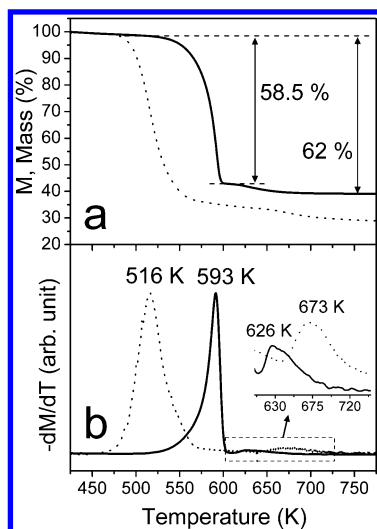


**Figure 4.** (a) TGA and (b) its first derivative traces of silver 4-nitrobenzoate (full lines); the dotted lines are for silver stearate.<sup>4d</sup>

group to silver in Ag-4NBA. All these spectral features nonetheless support the contention that the 4-NBA moiety is sustained at least up to 593 K without decomposition.

**3.2.2. TGA Measurement.** Figures 4a and 4b (see full lines) show the TGA and its first derivative traces of Ag-4NBA, respectively. For comparison, similar data for Ag-STA are also shown in the figures as dotted lines. It is evident that no mass loss occurs up to  $\sim 520$  K. This implies that the transition occurring at 383 K in Figure 3 is associated entirely with the conformational change in Ag-4NBA. In the temperature region of 520–775 K, two distinct mass loss features are observed in Figure 4. Most of the mass loss occurs around 593 K, and then a small amount is subsequently lost around 623 K. During the interval, the actual mass loss amounts to 58.5%. The first mass loss event is presumably associated with the formation of 4NBA-capped silver nanoparticles caused by the thermal decomposition of Ag-4NBA (vide infra), whereas the second loss event is due to the desorption of 4-NBA from the nanoparticles as well as the decomposition of residual free acid. On the basis of the formula weight of Ag-4NBA ( $\text{AgCO}_2(\text{C}_6\text{H}_4)\text{NO}_2$ ) and the data from the elemental analysis, if the organic moiety is completely lost, the mass loss has to amount to 62% in total. It is remarkable that this value is exactly the same as that observed by the TGA measurement. This indicates that free silver remains exclusively above 623 K.

It is intriguing that the first mass loss event occurs for Ag-4NBA at about 80 K higher temperature than for Ag-STA, whereas the second loss event occurs at about 50 K lower temperature (see the dotted lines in Figure 4; similar dotted data are also obtained for silver hydroxyhexadecanoate<sup>4f</sup>). Because the first mass loss event is associated with the formation of Ag nanoparticles, the higher temperature must be a result of the stronger Ag-COO bond in Ag-4NBA than Ag-STA. As mentioned previously, the stronger Ag-COO bond in Ag-4NBA has to be attributed to the conjugation effect of the carboxylate group to the aromatic ring as well as to the inter-ring  $\pi\pi$  interaction. Considering the fact that the second mass loss event is associated with the complete loss of organic moieties, the lower temperature in Ag-4NBA can be understood by presuming that the adsorption strength of 4-NBA on highly curved Ag nanoparticles is far smaller than that of STA. At higher temperatures, the inter-ring  $\pi\pi$  interaction will not be favorable for rigid aromatic molecules, whereas the vdW interaction is possible for flexible alkanolic acids.

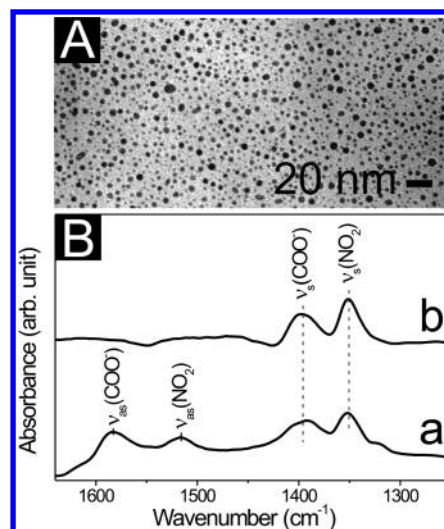


**Figure 5.** (A) TEM image of silver nanoparticles obtained from the thermal decomposition of silver 4-nitrobenzoate. (B) DRIFT spectrum of silver nanoparticles obtained from the thermal decomposition of silver 4-nitrobenzoate (a) and that of 4-nitrobenzoic acid self-assembled on 2  $\mu\text{m}$ -sized silver powder (b).

**3.2.3. Identity of the Thermal Decomposition Product of Ag-4NBA.** Recently, we have reported that alkanecarboxylate-derivatized silver nanoparticles with a uniform size distribution can be obtained via the thermal decomposition of silver alkanecarboxylates under  $\text{N}_2$  atmosphere.<sup>4d,4f,6</sup> In this light, consulting the DRIFT spectroscopy and TGA data, we have analyzed a sample of Ag-4NBA preheated to 600 K for 5 min in  $\text{N}_2$  atmosphere to verify that 4NBA-capped silver nanoparticles are indeed produced by the thermal decomposition of Ag-4NBA. The heated sample was rinsed thoroughly with ethanol to remove free acids or possible impurities. The remaining solid was soluble in a mixed solvent of chloroform and methanol. Figure 5A shows a typical TEM image of the sample. The image reveals that silver nanoparticles are indeed formed by the thermal decomposition of Ag-4NBA. The sizes of the nanoparticles are quite uniform with an average diameter of  $6.0 \pm 1.4$  nm. The formation of silver nanoparticles can also be confirmed from the XRD pattern (see the Supporting Information); all the XRD peaks can be attributed to the reflections of face-centered cubic Ag. We can confirm further from DRIFT spectroscopy that the silver nanoparticles are passivated with 4-nitrobenzoate. In the DRIFT spectrum of the silver nanoparticles shown in Figure 5B(a), peaks due to  $\nu_{\text{as}}(\text{COO}^-)$ ,  $\nu_{\text{as}}(\text{NO}_2)$ ,  $\nu_{\text{s}}(\text{COO}^-)$ , and  $\nu_{\text{s}}(\text{NO}_2)$  are clearly identified at 1583, 1516, 1395, and 1350  $\text{cm}^{-1}$ , respectively. The presence of these bands supports the contention that the silver nanoparticles are derivatized with 4-nitrobenzoate. One intriguing aspect is that only the  $\nu_{\text{s}}(\text{COO}^-)$  and  $\nu_{\text{s}}(\text{NO}_2)$  bands are identified in the DRIFT spectrum of 4-NBA on powdered silver shown in Figure 5B(b), whereas the  $\nu_{\text{as}}(\text{COO}^-)$  and  $\nu_{\text{as}}(\text{NO}_2)$  bands are also identified in the DRIFT spectrum of nanoparticles in Figure 5B(a). It has been well established that the usual IR surface selection rule is applicable even to the surface of fine metal particles.<sup>2c,11,13</sup> The appearance of the  $\nu_{\text{as}}(\text{COO}^-)$  and  $\nu_{\text{as}}(\text{NO}_2)$  bands in Figure 5B(a) may be indicative of the binding of 4-nitrobenzoate to Ag nanoparticles via only one of the two carboxylate oxygen atoms, whereas in the self-assembled monolayers (SAMs) of 4-NBA on powdered silver, the carboxylate group is bound to silver symmetrically via its two oxygen atoms. In fact, Merklin et al.<sup>14</sup> observed a similar spectral feature to that shown in Figure 5B(a) in their surface-enhanced IR absorption study of 4-NBA on silver island film, but the two antisymmetric bands, that is,  $\nu_{\text{as}}(\text{COO}^-)$  and

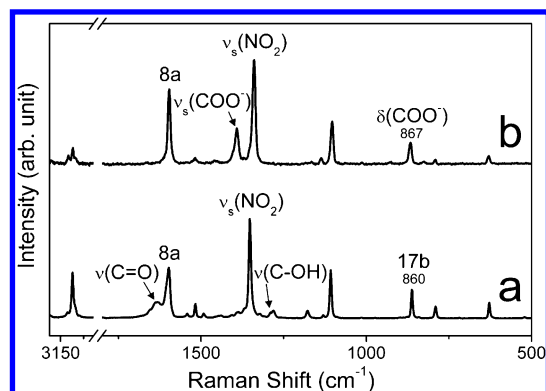


**Figure 6.** Raman spectra of (a) pure 4-nitrobenzoic acid and (b) silver 4-nitrobenzoate taken using the 514.5-nm line of an Ar<sup>+</sup> laser as the excitation source under spinning at 3000 rpm; the power at the sampling position was 17 mW, and the spectral acquisition time was 5 s.

$\nu_{\text{as}}(\text{NO}_2)$ , disappeared after thorough rinsing with methanol. In our work, however, the  $\nu_{\text{as}}(\text{COO}^-)$  and  $\nu_{\text{as}}(\text{NO}_2)$  bands barely disappeared in the DRIFT spectrum of the nanoparticles even after thorough rinsing with methanol and ethanol.

As mentioned in the previous section, free silver remains exclusively above 623 K (XRD data not shown). When such a thermal decomposition is conducted after coating Ag-4NBA on inflammable solid substrates, highly SERS-active, nanostructured Ag film can be fabricated as demonstrated in our previous publication.<sup>7</sup>

### 3.3. Photochemical Behavior of Silver 4-Nitrobenzoate.

Bokhonov et al.<sup>15</sup> reported that long-chain silver carboxylates were photochemically decomposed into silver nanoparticles under UV irradiation. Yonezawa et al.<sup>16</sup> showed that a silver film composed of silver clusters could be obtained from the photolysis of silver alginate under UV irradiation. These reports suggest that silver carboxylates can be transformed to nanosized silver particles upon irradiation by UV light. It is indeterminate, however, whether Ag nanoparticles can also be produced by the irradiation of visible light onto Ag-4NBA. If Ag nanoparticles are produced by visible-light irradiation, the organic moiety, that is, 4-NBA, may also be subjected to photochemical reaction. It can be expected from our recent SERS observations that the nitro-to-amine group conversion takes place for 4-NBT on nanostructured silver by irradiation with an Ar<sup>+</sup> laser at 514.5 nm.<sup>2a,2b</sup> The photoconversion efficiency was found to be highly dependent on the extent of surface roughness, that is, atomic- and nanoscale roughness, which is intimately associated with the SERS enhancement sites, that is, the chemical and electromagnetic enhancement sites, respectively.<sup>2b</sup> Separately, we found that the Ag nanoparticles physically in contact with 4-NBT SAMs on Au could also induce the photolytic reduction of the 4-NBT moiety simply by irradiation with 514.5-nm laser irradiation in ambient conditions.<sup>17</sup> Based on these observations, we have examined the visible-light response of Ag-4NBA by Raman spectroscopy.

Figures 6a and 6b show the ordinary Raman (OR) spectra of pure 4-NBA and Ag-4NBA, respectively, taken using the 514.5-nm line of an Ar<sup>+</sup> laser as the excitation source. During the measurement of the latter spectrum, a pelletized Ag-4NBA sample was spun at 3000 rpm in order to minimize any possible photoreaction. In the acid spectrum (Figure 6a), the  $\nu(\text{C}=\text{O})$  and  $\nu(\text{C}-\text{OH})$  bands derived from the H-bonded carboxylic group are clearly identified at 1636 and 1289  $\text{cm}^{-1}$ , respectively. The corresponding bands are completely absent in the Ag-4NBA spectrum. Instead, in Figure 6b, the  $\nu_{\text{s}}(\text{COO}^-)$  and  $\delta(\text{COO}^-)$  bands derived from the carboxylate group are observed at 1392

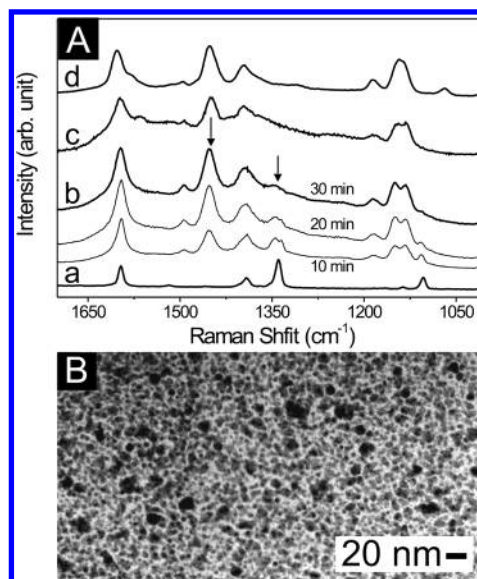


**Figure 7.** (A) Raman spectra of silver 4-nitrobenzoate taken at static conditions under irradiation by the 514.5-nm line (17 mW at the sampling position) for (a) 5 s and (b) 10, 20, and 30 min. (c) Raman spectrum of Ag-4ABA and (d) SERS spectrum of 4ABA adsorbed on 2  $\mu\text{m}$ -sized silver powder; both are obtained using the 514.5-nm line. The arrows in (b) denote the occurrence of distinct spectral changes. (B) TEM image of silver nanoparticles obtained from the photolysis of silver 4-nitrobenzoate.

and 867  $\text{cm}^{-1}$ , respectively, in agreement with the IR results (see the Supporting Information). (The fact that the  $\nu(\text{C}=\text{O})$  band for the free acid appears at very different positions in the IR and Raman spectra indicates that 4-NBA exists as a hydrogen-bonded dimer. This form has a center of symmetry so that when the two monomer compounds vibrate in phase, the vibration will be Raman-active only, and when they vibrate out-of-phase, the vibrations will be IR-active only. In the Raman spectrum, the symmetrical C=O stretch is thus seen near 1650  $\text{cm}^{-1}$ , and in the IR spectrum, the antisymmetrical C=O stretch is seen near 1700  $\text{cm}^{-1}$ .<sup>18</sup>)

The Raman spectral features of Ag-4NBA taken in static conditions were significantly different from those obtained in spinning conditions. In Figure 7A(b) are shown the Raman spectra of Ag-4NBA taken consecutively in static conditions under exposure by an Ar<sup>+</sup> laser at 514.5 nm for 10, 20, and 30 min; the sampling area was  $\sim 1 \mu\text{m}^2$ , and the power at the sampling position was 17 mW. For comparison, the Raman spectrum taken in spinning conditions (the same as that in Figure 6b) is reproduced in Figure 7A(a). Dramatic differences are identified in the spectral region of 1300–1500  $\text{cm}^{-1}$ . As indicated by the two arrows in Figure 7A(b), a peak near 1455  $\text{cm}^{-1}$  grows and becomes stronger while a peak at 1340  $\text{cm}^{-1}$  progressively weakens as the laser exposure time increases. Because the 1340  $\text{cm}^{-1}$  peak can be assigned to  $\nu_{\text{s}}(\text{NO}_2)$ , its decrease in intensity indicates that a certain photoreaction occurs at the nitro group of 4-NBA. The identity of the 1455  $\text{cm}^{-1}$  peak is rather uncertain at the moment. Nonetheless, because no spectral change occurs at all for the free acid, that is, 4-NBA, even after prolonged exposure to an Ar<sup>+</sup> laser, the spectral change in Figure 7A(b) must have been associated with the Ag ions in Ag-4NBA.

It is surprising that the Raman spectrum of Ag-4ABA obtained also in static conditions and shown in Figure 7A(c) is almost identical to that of Ag-4NBA in Figure 7A(b). Moreover, it is very noteworthy that these Raman spectral features resemble very closely the SERS spectral features of 4-ABA self-

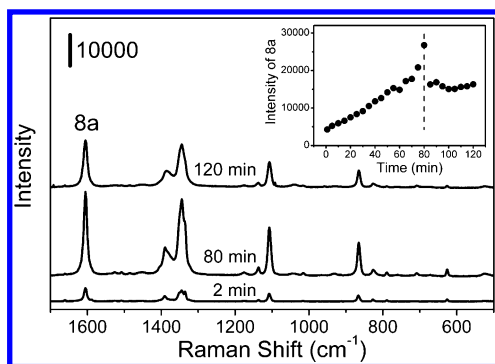


**Figure 8.** Raman spectra of silver 4-nitrobenzoate taken at static conditions under irradiation by the 632.8-nm line (17 mW at the sampling position) for different durations. The inset shows the variation of the 8a mode intensity of 4-NBA. The dashed line is drawn only as a guide to the eye.

assembled on the 2- $\mu\text{m}$ -sized silver powders shown in Figure 7A(d). These observations suggest that Ag nanoparticles have indeed been produced from Ag-4NBA upon irradiation by an  $\text{Ar}^+$  laser and that the nitro-to-amine group photoconversion has subsequently taken place on nanosized Ag particles.

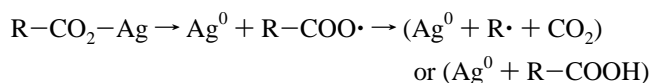
To confirm the production of nanosized silver particles, a piece of pelletized Ag-4NBA that had been exposed to the 514.5-nm line of a 17 mW  $\text{Ar}^+$  laser for 10 min was immersed in a chloroform/methanol mixture, and then the mixture was shaken gently after which its decanted solution was dropped on a copper grid for the TEM measurement; the white-colored Ag-4NBA turns yellowish-brown upon irradiation by an  $\text{Ar}^+$  laser. In fact, as can be seen in Figure 7B, nanosized silver particles are clearly observed. Contrary to the nanoparticles formed from the thermal decomposition of Ag-4NBA, the sizes are polydisperse and the shapes are quite irregular. Some particles are also seen to be present in a highly aggregated state. These data dictate that the spectra in Figure 7A(b) must be SERS spectra that have been derived from the photolysis of Ag-4NBA to give aggregated Ag nanoparticles followed by nitro-to-amine photoconversion on these particles.

To examine the possible wavelength dependence, the Raman spectrum of Ag-4NBA has also been obtained in static conditions using the 17 mW He/Ne laser at 632.8 nm as the excitation source. Figure 8 shows the Raman spectra obtained consecutively under exposure to the light for 2, 80, and 120 min. Surprisingly, the Raman spectral pattern is nearly invariant, although the absolute peak intensities are variable with respect to the time of laser exposure. The Raman spectral pattern in Figure 8 is seen to be comparable to that in Figure 6b. This implies that the nitro-to-amine group conversion does not take place for Ag-4NBA upon exposure to the He/Ne laser at 632.8 nm. Nonetheless, the changes in the absolute peak intensities in Figure 8 are indicative of the occurrence of some sort of photolysis. As shown in the inset of Figure 8, the peak intensity of the 8a mode gradually increases up to 80 min and then abruptly decreases and reaches a plateau level. These spectral changes are presumed to be associated with the production and aggregation of Ag nanoparticles by 632.8-nm radiation. We could indeed identify nanosized particles from the TEM measurement of the He/Ne laser exposed Ag-4NBA (data not shown). We separately confirmed that the nitro-to-amine group conversion hardly occurs for 4-NBA adsorbed on SERS-active Ag substrates by 632.8-nm radiation, as found in this work. This may reflect that photoelectrons are more readily ejected from Ag (at least in the visible region) as the wavelength of the light source becomes closer to that of the surface plasmon

resonance of silver. Regarding the latter matter, it has been observed by Fedurco et al.<sup>19</sup> that the surface roughening of Ag results in a drastic increase of the photocurrent for the wavelength close to the surface plasmon frequency. It is well conceivable that the condition of surface plasmon resonance can be satisfied with the 514.5-nm excitation by the aggregation of Ag nanoparticles. In particular, as shown in Figure 7B, when the photolyzed Ag nanoparticles are appropriately aggregated to show a large electromagnetic (EM) effect, the photoelectron ejection efficiency will reach such a level as to induce chemical reduction of the nearby functional group(s).

We have to mention that the SERS spectrum is not observable from the 4NBA-capped Ag nanoparticles produced via the thermal decomposition of Ag-4NBA; this is why only the DRIFT spectrum is shown in Figure 5B(a). This is in sharp contrast with the photolyzed Ag nanoparticles. This apparent difference can be understood by recalling the fact that the SERS effect is derived mostly from the EM enhancement that is in turn strongly associated with the sizes and shapes of nanoparticles as well as nanoaggregates.<sup>20</sup> As seen in Figure 5A, the thermally produced Ag nanoparticles are quite monodisperse whereas the photoproduced Ag nanoparticles in Figure 7B are highly irregular. It is presumed that at the initial stage of photolysis, very small Ag nanoparticles that are too small to exhibit SERS phenomenon are produced, but further exposure of light must lead to the growth and agglomeration of Ag nanoparticles sufficient for the occurrence of the SERS phenomenon. In contrast, during the thermal decomposition of Ag-4NBA, 4NBA-capped Ag nanoparticles are produced only in a limited temperature region so that the particles must assume well-separated positions without aggregation; hence, the EM enhancement is insufficient to produce the SERS phenomenon.

**3.4. Plausible Mechanism for Producing Silver Nanoparticles from Silver 4-Nitrobenzoate.** There is no generally accepted mechanism for the thermal as well as the photolytic decomposition of silver carboxylates. Nonetheless, it has been proposed in the literature that both processes must proceed via the production/annihilation of organic radicals as follows:<sup>15,16,21,22</sup>



The carboxyl radical ( $\text{R-COO}\cdot$ ) can either decompose into a secondary radical ( $\text{R}\cdot$ ) and carbon dioxide ( $\text{CO}_2$ ) or convert to polymeric species ( $\text{R}_n$ ) and/or carboxylic acid ( $\text{RCOOH}$ ) by hydrogen abstraction from nearby organic moieties.

In the present work, the thermal decomposition of Ag-4NBA was observed to occur above 593 K under  $\text{N}_2$  atmosphere. The  $\text{C=O}$  stretching peak was clearly identified at  $\sim 1700 \text{ cm}^{-1}$  above 513 K (see Figure 3), which must have arisen from a free acid, that is, 4-NBA. (To form a free acid, a hydrogen source is required. Its source is not yet clear, but we presume that hydrogen atoms are provided by the dehydrogenation of phenyl rings.) Metallic silver was also found to form upon thermal decomposition of Ag-4NBA. However, we could not find any evidence that would indicate the presence of silver oxide as a constituent of the thermal decomposition products. This implies that metallic silver and 4-NBA are produced as the primary decomposition products but metallic silver is immediately stabilized as nanoparticles by capping with 4-NBA molecules, as shown in Figure 5B.

Although the photolysis of Ag-4NBA was conducted in the ambient condition, its reaction appeared to proceed via a

mechanism similar to thermolysis. As mentioned previously, Yonezawa et al.<sup>16</sup> prepared a silver film via the photolysis of silver alginate on glass under UV irradiation in air; the film was confirmed to be composed of pure silver by XRD and X-ray fluorescence (XRF) analyses. The absence of silver oxide may indicate that water molecules in air do not participate in the photolysis of silver alkanecarboxylates (AgCO<sub>2</sub>R). We presume that the conditions of inertness of water and/or ambient oxygen are maintained even for the cases of photolysis by visible light. It is also expected that the irradiation by visible light does not cause noticeable damage to the organic moiety of AgCO<sub>2</sub>R. In this light, it is not unreasonable to observe that 4NBA-capped Ag nanoparticles are produced by the visible-light-induced photolysis of Ag-4NBA. Once the 4NBA-capped Ag nanoparticles are formed, they will be immediately subjected to surface-induced photoreaction to form 4ABA-capped Ag nanoparticles.

Regarding the surface-induced photoreaction of 4-NBT or 4-NBA on Ag, two specific questions have to be answered, namely, how the reaction proceeds, and what the hydrogen source is. Although the detailed mechanism is a matter of conjecture, the reaction is presumed to be associated with the charge transfer from silver to the adsorbed molecule. If the energy difference between the Fermi level of the metal and the low-lying excited state of the charge-transfer complex matches the energy of the excitation radiation, a resonant charge transfer from the metal to the excited state of the complex can take place.<sup>1b</sup> The electron-transfer step is supposed to be a direct, optically induced charge transfer from the Fermi level to the lowest-lying unoccupied molecular orbital of the adsorbate–silver complex. On the other hand, it is known that when photoreaction occurs for aromatic nitro molecules in a solution phase, a chemical species from which hydrogen atom(s) can be abstracted is needed.<sup>23</sup> For a similar photoreaction to occur in air, water has been claimed to act as a hydrogen source.<sup>24</sup> The photoreaction of 4-NBT on Ag occurs several times faster in water or ethanol medium than in air.<sup>2a</sup> The photoreaction of 4-NBA occurs much faster when the molecule is coadsorbed on Ag with hydrophilic group-terminated alkanethiols than with hydrophobic group-terminated alkanethiols.<sup>2c</sup> These observations suggest that the source of hydrogen atoms in the surface-induced photoreaction of 4-NBT on Ag to 4-ABT must be water or solvent molecules trapped inside the 4-NBT monolayers rather than 4-NBT itself.

#### 4. Conclusion

We confirmed by XRD analysis that silver 4-nitrobenzoate (Ag-4NBA) consisted of a layered structure. The temperature-dependent DRIFT and TGA measurements indicated that Ag-4NBA was subjected to three distinct transitions. In the first transition at 383 K, the binding state of carboxylate is converted from bridging to unidentate. In the second transition at 593 K, Ag-4NBA is decomposed to produce 4NBA-capped Ag nanoparticles. This second transition temperature for Ag-4NBA is about 80 K higher than that for silver alkanecarboxylates, and such enhanced thermal stability of Ag-4NBA must be associated with the conjugation of the carboxylate group to the aromatic ring. In the third transition at 623 K, the organic moieties are totally lost from the Ag nanoparticles. Separately, SERS-active, nanosized silver particles or aggregates were produced from Ag-4NBA by visible-laser irradiation at 514.5 and 632.8 nm. The particles produced under irradiation by the 514.5-nm light were derivatized with 4-ABA, whereas those under the 632.8-nm light were capped with 4-NBA. The nitro-to-amine group conversion observed herein is exactly in conformity with the recent SERS

study of 4-NBA; hence, 4ABA-capped Ag nanoparticles are produced via the formation of 4NBA-capped Ag nanoparticles from Ag-4NBA. From the point of view of application, all of these observations suggest that, if the terminal functionality of the precursor molecule is judiciously chosen, the silver nanoparticles derivatized with proper end-functional molecules can be synthesized not only via thermolysis but also by photolysis of silver carboxylates. For instance, amine group-terminated nanoparticles can be easily manufactured via such thermolysis and/or photolysis, and the amine group may further be modified to incorporate other molecules or biomolecules to function as delicate indicators or biosensors. In addition, the wavelength-dependent photoresponse of Ag-4NBA can be applied to the read-out methodology in memory devices and/or sensor fields.

**Acknowledgment.** This work was supported in part by the Ministry of Health & Welfare (Korea Health 21 R&D Project 01-PJ11-PG9-01NT00-0023) and by the Ministry of Science and Technology (Nano Project, M10213240001-02B1524-00210) in the Republic of Korea.

**Supporting Information Available:** Room-temperature DRIFT spectrum of silver 4-nitrobenzoate; XRD pattern of silver nanoparticles obtained from the thermal decomposition of silver 4-nitrobenzoate. This material is available free of charge via the Internet at <http://pubs.acs.org>.

#### References and Notes

- (1) (a) Roth, P. G.; Venkatachalam, R. S.; Boerio, F. J. *J. Chem. Phys.* **1986**, *85*, 1150. (b) Sun, S.; Birke, R. L.; Lombardi, J. R.; Leung, K. P.; Genack, A. Z. *J. Phys. Chem.* **1988**, *92*, 5965. (c) Bercegol, H.; Boerio, F. J. *J. Phys. Chem.* **1995**, *99*, 8763. (d) Yang, X. M.; Yang, X. M.; Tryk, D. A.; Hashimoto, K.; Fujishima, A. *J. Phys. Chem. B* **1998**, *102*, 4933.
- (2) (a) Han, S. W.; Lee, I.; Kim, K. *Langmuir* **2002**, *18*, 182. (b) Lee, S. J.; Kim, K. *Chem. Phys. Lett.* **2003**, *378*, 122. (c) Han, H. S.; Han, S. W.; Kim, C. H.; Kim, K. *Langmuir* **2000**, *16*, 1149.
- (3) (a) Aksay, I. A.; Trau, M.; Manne, S.; Honma, I.; Yao, N.; Zhou, L.; Fenter, P.; Eisenberger, P. M.; Gruner, S. M. *Science* **1996**, *273*, 892. (b) Lacroix, P. G.; Clement, R.; Nakatani, K.; Zyss, J.; Ledoux, I. *Science* **1994**, *263*, 658. (c) Vermeulen, L. A.; Thompson, M. E. *Nature* **1992**, *358*, 656. (d) Laget, V.; Hornick, C.; Rabu, P.; Drillon, M.; Turek, P.; Ziessel, R. N. *Adv. Mater.* **1998**, *10*, 1024. (e) Kagan, C. R.; Mitzi, D. B.; Dimitrakopoulos, C. D. *Science*, **1999**, *286*, 945. (f) Mitzi, D. B. *Chem. Mater.* **2001**, *13*, 3283.
- (4) (a) Vand, V.; Aitken, A.; Campbell, R. K. *Acta Crystallogr.* **1949**, *2*, 398. (b) Matthews, F. W.; Warren, G. G.; Michell, J. H. *Anal. Chem.* **1950**, *22*, 514. (c) Tolochko, B. P.; Chernov, S. V.; Nikitenko, S. G.; Whitcomb, D. R. *Nucl. Instrum. Methods A* **1998**, *405*, 428. (d) Lee, S. J.; Han, S. W.; Choi, H. J.; Kim, K. *J. Phys. Chem. B* **2002**, *106*, 2892. (e) Lee, S. J.; Han, S. W.; Choi, H. J.; Kim, K. *J. Phys. Chem. B* **2002**, *106*, 7439. (f) Choi, H. J.; Han, S. W.; Lee, S. J.; Kim, K. *J. Colloid Interface Sci.* **2003**, *264*, 458.
- (5) (a) Uvarov, N. F.; Burleva, L. P.; Mizen, M. B.; Whitcomb, D. R.; Zou, C. *Solid State Ionics* **1998**, *107*, 31. (b) Chadha, M.; Dunnigan, M. E.; Sahyun, M. R. V.; Ishida, T. *J. Appl. Phys.* **1998**, *84*, 887.
- (6) Lee, S. J.; Han, S. W.; Kim, K. *Chem. Commun.* **2002**, 442.
- (7) Lee, S. J.; Kim, K. *Chem. Commun.* **2003**, 212.
- (8) Blakeslee, A. E.; Hoard, J. L. *J. Am. Chem. Soc.* **1956**, *78*, 3029.
- (9) Groth, P. *Acta Chem. Scand. A* **1980**, *34*, 229.
- (10) *CRC Handbook of Chemistry and Physics*, 71st ed.; Lide, D. R., Ed.; CRC Press: Boca Raton, FL, 1990.
- (11) Lee, S. J.; Han, S. W.; Yoon, M.; Kim, K. *Vib. Spectrosc.* **2000**, *24*, 265.
- (12) (a) Gericke, A.; Hühnerfuss, H. *Thin Solid Films* **1994**, *245*, 74. (b) Ohe, C.; Ando, H.; Sato, N.; Urai, Y.; Yamamoto, M.; Itoh, K. *J. Phys. Chem. B* **1999**, *103*, 435.
- (13) Han, H. S.; Kim, C. H.; Kim, K. *Appl. Spectrosc.* **1998**, *52*, 1047; Lee, S. J.; Kim, K. *Vib. Spectrosc.* **1998**, *18*, 187; Han, S. W.; Han, H. S.; Kim, K. *Vib. Spectrosc.* **1999**, *21*, 133.
- (14) Merklin, G. T.; Griffith, P. G. *J. Phys. Chem. B* **1997**, *101*, 5810.
- (15) Bokhonov, B. B.; Lomovsky, O. I.; Andreev, V. M.; Boldyrev, V. V. *J. Solid State Chem.* **1985**, *58*, 170; Bokhonov, B. B.; Burleva, L. P.; Whitcomb, D. R.; Usanov, Yu. E. *J. Imaging Sci. Technol.* **2001**, *45*, 259.

(16) Yonezawa, Y.; Takami, A.; Sato, T.; Yamamoto, K.; Sasanuma, T.; Ishida, H.; Ishitani, A. *J. Appl. Phys.* **1990**, *68*, 1297; Yonezawa, Y.; Konishi, Y.; Hada, H.; Yamamoto, K.; Ishida, H. *Thin Solid Films* **1992**, *218*, 109.

(17) Kim, K.; Lee, I.; Lee, S. J. *Chem. Phys. Lett.* **2003**, *377*, 201.

(18) Lin-Vein, D.; Colthup, N. B.; Fateley, W. G.; Grasselli, J. G. *The Handbook of Infrared and Raman Characteristic Frequencies of Organic Molecules*; Academic Press: San Diego, CA, 1991.

(19) Fedurco, M.; Shklover, V.; Augustynski, J. *J. Phys. Chem. B* **1997**, *101*, 5158.

(20) (a) Kneipp, K.; Kneipp, H.; Itzkan, I.; Dasari, R. R.; Feld, M. S. *J. Phys.: Condens. Matter* **2002**, *14*, R597 and references therein. (b) Shipway, A. N.; Katz, E.; Willner, I. *ChemPhysChem*, **2000**, *1*, 18.

(21) Field, E. K.; Meyerson, S. *J. Org. Chem.* **1976**, *41*, 916.

(22) Usabaliev, B. T.; Nadjafov, H. N.; Musaev, A. A.; Mamedov, K. S. *Thermochim. Acta* **1989**, *93*, 57.

(23) Barltrop, J. A.; Bunce, N. J. *J. Chem. Soc. C* **1968**, 1467.

(24) Tsai, W.-H. Ph.D. Dissertation, University of Cincinnati, Cincinnati, OH, 1991.